Core-Selective Switch for SDM Network based on LCPG and MEMS technology

Yuki Kuno, Masahiro Kawasugi, Yuji Hotta, Ryohei Otowa, Makoto Mizoguchi, and Yasuki Sakurai*
SANTEC CORPORATION, 5823 Ohkusa-nenjozaka, Komaki 485-0802 Japan
**ysakurai@santec-net.co.jp*

Abstract: We propose a core selective switch (CSS) with VOA function utilizing liquid crystal polarization grating and MEMS technology. The prototype of 19-core 1×8 CSS showed an attenuation of 19.5 dB with more than 35 dB optical crosstalk. © 2022 The Authors

1. Background

In optical communications, innovative technologies are required to meet the demand for large-capacity communications beyond the fifth generation (5G) systems [1]. One of the representative technologies is spatial-division multiplexing (SDM) using multi-core fibers (MCFs) [2-3]. We proposed the construction of an SDM layer using MCF in addition to a conventional wavelength division multiplexing (WDM) layer, which has high scalability and provides superior economical performance [4]. In spatial cross-connect (SXC) on an SDM layer, a fan-in/fan-out (FIFO) device is typically required to branch an MCF to a single-core fiber (SMF); however, this architecture may be inefficient, especially as the number of SMF-based devices, such as optical switches, increases with increasing core count of the MCF. A core selective switch (CSS) that capable of branching multiple MCFs without an FIFO device, as shown in Figure 1, has been proposed and demonstrated. Studies on 5-core [5], 3 bundles of 5-core [6], and 19-core MCF [7] have been reported till date.

Typically, optical cross-connect (OXC) or reconfigurable add-drop (ROADM) switches have a built-in variable optical attenuator (VOA) function to adjust optical gain, such as wavelength selective switch (WSS) in a WDM network. In SXC, realizing VOA sensibly is a significant challenge, especially for massive core MCFs, because of the need to minimize optical crosstalk with tight core spacing. One method to add the VOA function is to adjust the amount of beam incident on the fiber core by controlling the tilted angle of the microelectromechanical system (MEMS) mirror [8]; however, concerns about the occurrence of excessive inter-core crosstalk in the MCF may exist. In addition, the wavelength-dependent loss and polarization-dependent loss of the MEMS tilted mirror VOA increase along with attenuation. A liquid crystal polarization grating (LCPG) has a periodic structure in the molecular orientation of a liquid crystal and generates diffraction due to optical anisotropy [9–11] without an optical beam displacement, as in a MEMS tilted mirror. Typically, LCPG has a structure, as shown in Figure 2, in which the molecular orientation direction is continuously modulated in one dimension and the diffraction is separated into right-handed circularly polarized (RCP) and left-handed circularly polarized (LCP) light. When a large voltage is applied to the liquid crystal, all the molecules align in the direction of the electric field and lose their diffraction-grating characteristics. In addition, the optical power of the diffraction can be changed depending on the applied voltage. Because the optical power of the 0^{th} order output is in a constant ratio to the input power, regardless of the input polarization, it can be used as a polarization-insensitive attenuator.

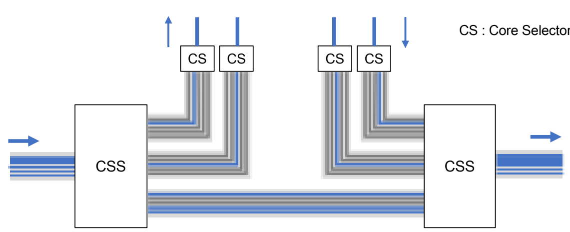

Fig. 1. Schematic architecture of SXC using CSS (Simplified)

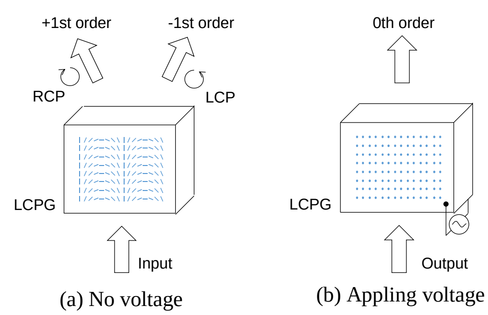

Fig. 2. LCPG operation principle

2. Design of LCPG-integrated CSS

A schematic of the designed 19-core fiber 1 × 8 CSS is shown in Figure 3. The optical system is a 4-f system, and a 19-core array was projected with a magnification factor $M = (f_2/f_1)$. Here, f_1 = 0.81 mm, f_2 = 50 mm, and M = 61.5. The core pitch of the MCF was 40 μm, and the optical beam pitch on the MEMS mirror plane was magnified to 0.04

× 61.5 = 2.46 mm. The optical signal from the input MCF can be output to any output MCFs by controlling the MEMS mirror angle. The LCPG for the VOA function can be inserted between the condenser lens and the MEMS mirror array and independently controlled on each channel, as shown in Figure 5.

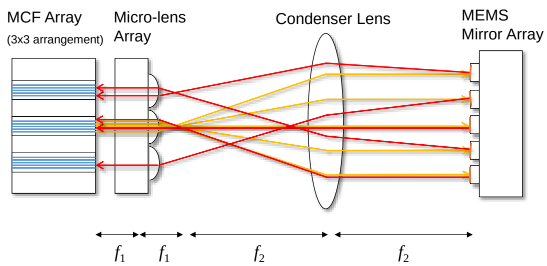

Fig. 3. Schematic diagram of CSS

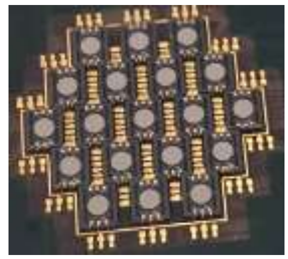
Fig. 4. MEMS mirror array

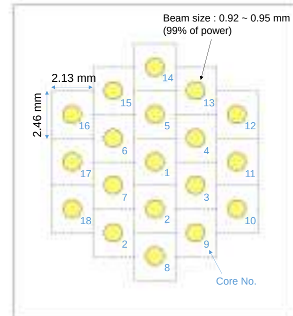

Fig. 5. Design of LCPG

The 1st order beam, an unwanted component, may cause inter-core or inter-port crosstalk. Therefore, it is desirable to be effectively diffracted at as large an angle as possible so as not to couple to fiber cores. However, a large diffraction angle requires a small lattice period for LCPG, which is limited by the elasticity of the liquid crystal. An aperture plate with an optical absorption layer was placed in front of the MEMS mirror array to eliminate the 1st order beam efficiently without requiring a large diffraction angle, as shown in Figure 6. The 1st order diffraction angle θ of the LCPG was set to 3.5° at 1550 nm. The lattice period was 25.3 µm, which was derived using λ / tan θ. The distance from the LCPG to the MEMS mirror array was 21 mm. Although the 1st order beam was also generated by the LCPG in the return path, it was sufficiently separated from the MCF array and did not affect the crosstalk.

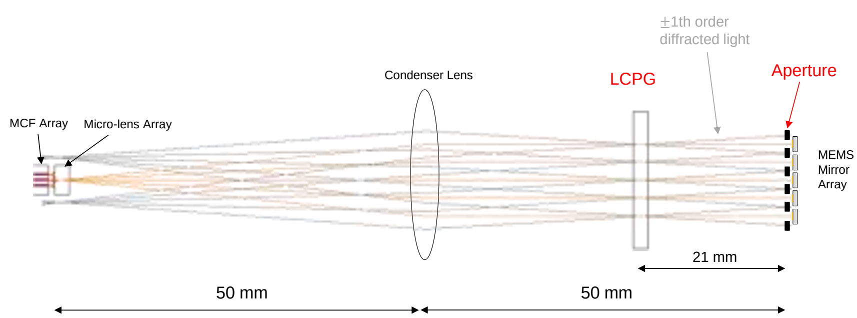

Fig. 6. Optical geometric design of LCPG integrated CSS.

3. Experiment

For the liquid crystal (LC) of LCPG, ZLI-4792 (Δn = 0.09, $\Delta\varepsilon$ = 5.3) from Merck was deployed, and the cell gap d was set as 12.5 µm. At this time, an indium-tin oxide (ITO) film was deposited on the entire surface of the glass substrate for single-channel operation. The retardation amount at λ = 1550 nm could be adjusted by controlling the applied voltage and matched completely with the condition of the disappearance of the 0th order beam given by $\Delta nd = \lambda/2$ (from equation (1) of [9]). A photocrosslinkable polymer was used as the LC alignment layer, and a periodic orientation lattice was patterned by optical holographic exposure. A lattice period of 24 µm was measured using a polarization microscope, as shown in Figure 7, which corresponds to a diffraction angle of 3.7°. When a collimated beam at 1550 nm was experimentally illuminated over the LCPG, the measured diffraction angle showed good agreement with the calculation. The measured 0th order transmission loss of the LCPG with an applied voltage of 15 $V_{p\text{-}p}$ was approximately 1.0 dB.

The LCPG was inserted in accordance with the configuration shown in Figure 6, and some optical characteristics were measured using unpolarized light. The extinction ratio was 19.5 dB, as shown in Figure 8, which was limited by the imperfection of the lattice owing to fabrication errors. Further improvement of the extinction ratio could be expected with process optimization of the LCPG. The minimum insertion loss within the measured voltage range was 4.7 dB. The transmission spectra over the entire C-band with various attenuations are shown in Figure 9. The spectral ripple could have been caused by the lack of an AR coating on the surface of the LCPG. The measured optical crosstalk between the cores and ports is shown in Figure 10. An inferior value was observed for all cores on Port-1 owing to an inter-core crosstalk of the MCF itself. The net crosstalk without the MCF characteristic was over 35 dB for all cores.

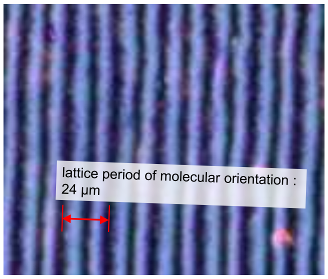

Fig. 7. LCPG image by polarization microscope

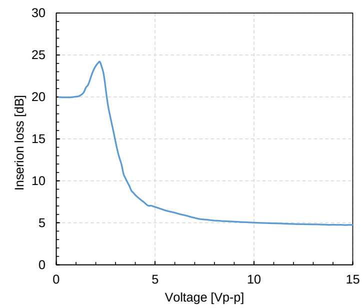

Fig. 8. Measured LCPG attenuation curve

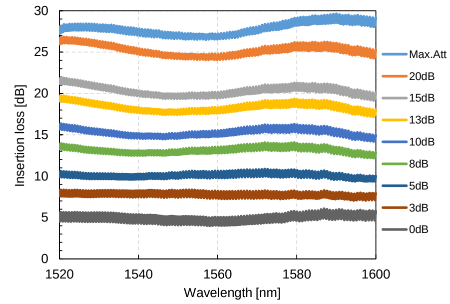

Fig. 9. Measured CSS transmission spectra

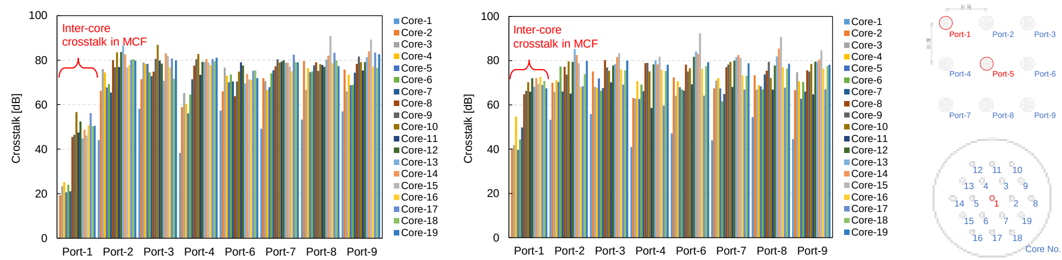

(a) $V_{p\text{-}p}$ = 2.04 V (Max Att.) (b) $V_{p\text{-}p}$ = 15 V (Att. 0dB)

Fig. 10. Measured optical crosstalk at all ports and cores (λ = 1550 nm, Input : Port-5 Core-1, Output : Port-1 Core-1)

4. Conclusion

We proposed and demonstrated a 19-core 1×8 CSS with VOA function-based LCPG and MEMS technology. The minimum insertion loss of 4.7 dB and an attenuation of 19.5 dB was observed with an applied voltage of 15 $V_{p\text{-}p}$. Even in the 19-core massive MCF switch configuration, the measured crosstalk was over 35 dB, owing to the LCPG operation principle. We believe that the proposed concept will contribute to the development of a new class of optical telecommunication networks.

Acknowledgments

This work was supported in part by National Institute of Information and Communication Technology (NICT) (Grant Number 00201). The authors are also grateful to Jinno Laboratory, Kagawa University (for valuable advice and discussion), Furukawa Electric Co., Ltd. (for the provision of MCF and FIFO), and Ono & Sakamoto Laboratory, Nagaoka University of Technology (for the provision of LCPG).

References

[1] B. Coll-Perales, J. Gozalvez, and J. L. Maestre, “5G and Beyond: Smart Devices as Part of the Network Fabric,” IEEE Network, vol. 33, pp. 170-177, Feb 2019.
[2] A. Muhammad, G. Zervas, D. Simeonidou and R. Forchheimer, "Routing, spectrum and core allocation in flexgrid SDM networks with multi-core fibers," 2014 International Conference on Optical Network Design and Modeling, 2014, pp. 192-197.
[3] T. Gonda et al., "Design of Multicore Fiber Having Upgradability From Standard Single-Mode Fibers and Its Application," in Journal of Lightwave Technology, vol. 37, no. 2, pp. 396-403, 15 Jan.15, 2019, doi: 10.1109/JLT.2019.2895903. vol. 37, no. 2, pp. 396-403, 2019.
[4] M. Jinno, T. Kodama, and T. Ishikawa, "Principle, design, and prototyping of core selective switch using free-space optics for spatial channel network," J. Lightw. Technol., vol. 38, no. 18, pp. 4895-4905, 2020.
[5] M. Jinno, I. Urashima, T. Ishikawa, T. Kodama, and Y. Uchida, "Core selective switch with low insertion loss over ultra-wide wavelength range for spatial channel networks," J. Lightwave Technol., vol. 40, no. 6, pp. 1821-1828, 2022.
[6] Y. Uchida, T. Ishikawa, I. Urashima, S. Murao, T. Kodama, Y. Sakurai, R. Sugizaki, and M. Jinno, "Core selective switch supporting 15 cores per port using bundled three 5-core fibers," Optical Fiber Communications Conference and Exhibition (OFC), M4J.2, 2022.
[7] Y. Kuno, M. Kawasugi, Y. Hotta, R.Otowa, M. Mizoguchi, F.Takahashi, Y. Sakurai, and M. Jinno, "19-core 1×8 Core Selective Switch for Spatial Cross-Connect," 2022 27th OptoElectronics and Communications Conference (OECC) and 2022 International Conference on Photonics in Switching and Computing (PSC), WE3-2, 2022
[8] K. Isamoto, K. Kato, A. Morosawa, Changho Chong, H. Fujita and H. Toshiyoshi, "A 5-V operated MEMS variable optical attenuator by SOI bulk micromachining," in IEEE Journal of Selected Topics in Quantum Electronics, vol. 10, no. 3, pp. 570-578, May-June 2004
[9] E. Nicolescu, . Mao, A. Fardad and M. Escuti, "Polarization-Insensitive Variable Optical Attenuator and Wavelength Blocker Using Liquid Crystal Polarization Gratings," in Journal of Lightwave Technology, vol. 28, no. 21, pp. 3121-3127, Nov.1, 2010
[10] H. Ono, A. Emoto, F. Takahashi, N. Kawatsuki, and T. Hasegawa, “Highly stable polarization gratings in photocrosslinkable polymer liquid crystals”, Journal of Applied Physics, vol. 94, no. 3, pp. 1298–1303, 2003
[11] C. Oh and M. J. Escuti, “Numerical analysis of polarization gratings using the finite-difference time-domain method”, Physical Review A, vol. 76, no. 4, 2007